

An integrated strategy for variational analysis of compliant  
plastic assemblies on shell elements

*Original*

An integrated strategy for variational analysis of compliant  
plastic assemblies on shell elements / Moos, Sandro; Vezzetti, Enrico. - In: INTERNATIONAL JOURNAL, ADVANCED  
MANUFACTURING TECHNOLOGY. - ISSN 0268-3768. - (2013). [10.1007/s00170-013-5080-0]

*Availability:*

This version is available at: 11583/2507680 since: 2016-02-18T17:27:53Z

*Publisher:*

Springer

*Published*

DOI:10.1007/s00170-013-5080-0

*Terms of use:*

This article is made available under terms and conditions as specified in the corresponding bibliographic description in  
the repository

*Publisher copyright*

(Article begins on next page)

NOTICE: this is the author's version of a work that was accepted for publication in "International Journal of Advanced Manufacturing Technology". Changes resulting from the publishing process, such as peer review, editing, corrections, structural formatting, and other quality control mechanisms may not be reflected in this document. Changes may have been made to this work since it was submitted for publication. A definitive version was subsequently published in:

The International Journal of Advanced Manufacturing Technology, Vol. 61, Issue 1-4, pp. 875-890. An integrated strategy for variational analysis of compliant plastic assemblies on shell elements. Springer London, 01/10/2013, DOI: 10.1007/s00170-013-5080-0.

The final publication is available at [link.springer.com](http://link.springer.com)

# An integrated strategy for variational analysis of plastic compliant assemblies on shell elements

Moos Sandro · Vezzetti Enrico

Received: date / Accepted: date

**Abstract** The variational analysis on compliant assembly has been shown to be significantly influenced by plastic deformation of the part's material induced by resistance spot welding and fixturing.

The aim of this paper is to define the FEM methods required to translate the complex interaction best described by a coupled thermo-electrical-mechanical simulation with solid elements to a shell model suitable for variational analysis.

The methods are here described and implemented into FEM run-time routines to be later used for the calculation of the influence coefficient matrixes and Monte-Carlo simulation, so to reduce the problem complexity.

The methods tested on the geometry of a butt joint are in good agreement with the results of more traditional FEM setup and reduce the computational effort for the variational analysis.

**Keywords** Compliant assembly · FEM · Variational analysis · Quality · Resistance spot welding · Plasticity

## 1 Introduction

In the automotive sector, many compliant parts are joined together to form the body assembly following typical steps that consist in loading and clamping the parts on fixtures, so to locate and orient them accordingly to the product's design, then applying the Resistance Spot Welding (RSW) process by mean of manual or robotic welding guns.

To guarantee the proper dimensional and geometrical properties of the manufacuted parts, required for the following assembly, hinged panel fitting and final assembly phases, the industries adopting an orientation towards continuous quality improvement also focus their attention on predicting the effects of the joining process on the final assembly dimensional quality, so to evaluate the overall process capability. (Chase et al. [1], Maropoulos et al. [2]).

Many works can be found in literature regarding tolerance stack-up applied to elastic compliant assemblies, passing through FEM to compute deformations and through Monte Carlo simulation to perform the statistical analysis. They are based on the influence coefficient method proposed by Liu et al. [3] which has the aim of extracting from a FEM analysis a linear relationship between the part's deviation vector and the assembly elastic springback.

Considering that each part is subjected to source of variation that will be forced to the nominal position by the clamps, the relationship between the deviation vector and the parts' reacting forces is established in the FEM but generally it's not returned to the user. So the sensitivity matrixes have been derived applying a unit force to each source of variation, directed as the variation and calculating the corresponding parts deformation and ordering them in a vector.

The elastic springback for the assembled structure is determined by the assembly stiffness matrix considering it as subjected to a force equal and opposed to those required to close the parts.

These relations are valid only for small deformation in elastic range but are linearly used for general variation vectors determined with the Monte Carlo simulation, so to allow a statistical description of the tolerance stack-up.

A detailed application of the influence coefficient, in the aerospace field, can be found in Byungwoo et al., which presented in [4] an approach to integrate the Datum Flow Chain

---

Moos Sandro · Vezzetti Enrico  
Politecnico di Torino – Dipartimento di Ingegneria Gestionale e della  
Produzione (DIGEP).  
Tel.: +39-11-5647294  
Fax: +39-11-5647299  
E-mail: sandro.moos@polito.it

analysis with a commercial 3D variation analysis software and FEA.

The first step is to define the compliance and sensitivity matrix of each parts by means of influence coefficients. The sensitivity matrix is computed once for all by FEM, with the parts located on a set of isostatic locators and then applying an unit displacement to the overconstrained joint at each part. The forces and deformations are calculated as (1a) (1b). The resulting force acting at joints is equal and opposite to the sum of the forces used to bend the parts in that position (1c) and this will be applied to the assembly in nominal condition to evaluate its springback. The compliance matrix of the whole assembly is computed in 1d applying a unit force on each joint and, finally, the displacement resulting on the control points can be defined as a linear combination of the effects computed on parts and assembly as in 1e.

$$\{F_i\} = [K_{vi}] \{V_i\} \quad (1a)$$

$$\{d_{pi}\} = [K_{pi}]^{-1} \{f_{pi}\} = [S_{pi}] \{V_i\} \quad (1b)$$

$$\{f_a\} = -\sum_i \{f_{pi}\} \quad (1c)$$

$$\{d_a\} = [K_a]^{-1} \{f_a\} = -[K_a]^{-1} \sum_i [K_{vi}] \{V_i\} = -\sum_i [S_{ai}] \{V_i\} \quad (1d)$$

$$\{u\} = \{u_0\} + \{d_p\} + \{d_a\} = \{u_0\} + \sum_i ([S_{pi}] - [S_{ai}]) \{V_i\} \quad (1e)$$

The approach allows the reduction of the computational time because the stiffness matrix is calculated once for all with influence coefficients and it is later used for statistical variation calculation with Monte Carlo simulation to calculate the probability functions and their contributors.

The equations 1 shows that the first step to define the compliance matrixes is to deform the parts with the unit displacements and to measure the displacement field.

The main drawback of those work is the use of a linear elastic model for the part's material, in fact the works of Feulvarch et al. [5], Hou et al. [6], Ranjbar et al. [7], Eisazadeh et al. [8] showed the presence of plastic deformations and a stress distribution inside and around the welding nugget, resulting after the thermal transformation caused by the welding current.

The previous work of Moos et al. [9] showed that, starting from welding flanges which are subjected to tolerances, the weldgun closure can cause relative sliding motion between the two flanges that are made permanent by the weld spot and that the deformations imposed by fixtures and electrodes before the weld cycle, also cause plasticization away from the welding spot, near bending fillets and locators. The comparison of the spingback of a butt joint calculated with the same boundary conditions, changing only the material model form elastic to plastic, also showed completely different behaviors.

As a further description of the result in [9], for a butt joint with a tolerance interference condition that hinders the correct loading on fixture, in figure 1 have been reproduced the total elastic strain energy density field after the clamps and the electrodes closure (fig.1a), after the thermal cycle

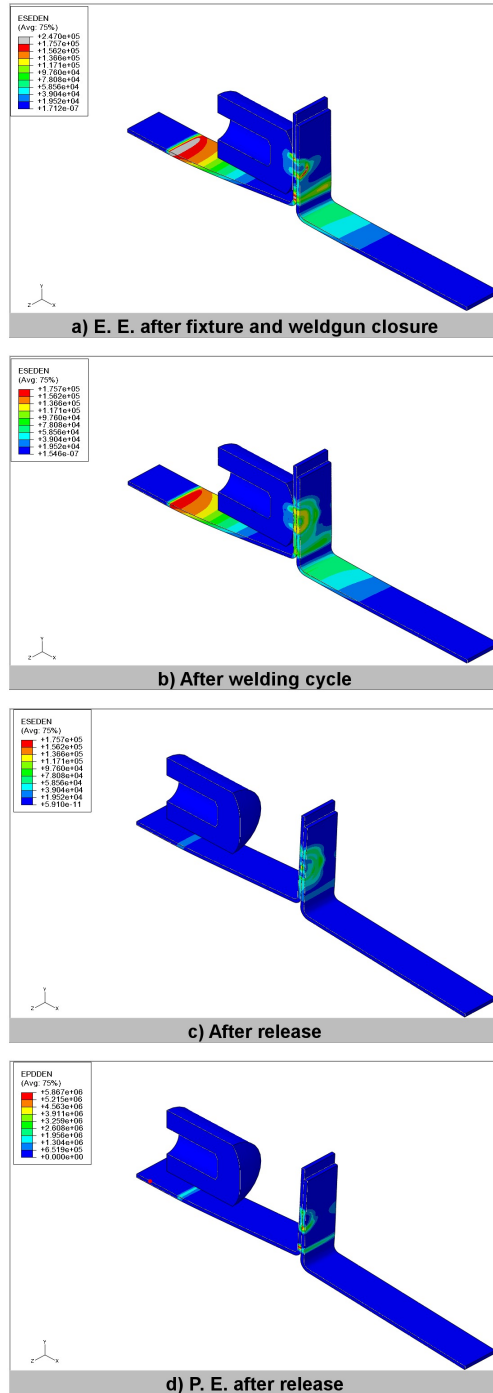


**Fig. 1** Elastic strain energy density. a) After fixture and weldgun closure. b) At the end of the welding cycle. c) After the fixture release. d) Total plastic energy per unit volume after fixture release.

(fig.1b) and after releasing (fig.1c), while figure fig.1d displays the total energy dissipated per unit volume in the element by plastic deformations after releasing.

Comparing figures 1a and 1b it's evident the reduction of the elastic energy stored by the initial deformations caused by the thermal cycle, particularly near the rear side of the

sheets where locators are positioned, at the base of the flanges and around the welding electrodes which are forcing together the sheets.

The remaining energy (fig.1b), will cause the assembly springback once released, so to reach the condition of fig.1c in which are evident the effects of the residual stresses near the weld nugget, the fillets at the flange's base and near the locators. In this released configuration, fig.1d displays that in those region also occurred material plasticization.

These results suggest that a more detailed modelization of the welding process should consider a plastic material model, because it is more suited to predict the deformation modes of the parts.

An approach in this direction was implemented by Fan et al. [10], who “superimposed” the local spot welding plastic distortions to a nominal FE assembly mesh, with welding flanges in matching condition. The simulation predicted the same mode of deformation experimentally measured on real parts: a distortion of the assembly with a twist induced around a diagonal axis, but underestimated the magnitude.

The deformations measured on the assembly were also compared with the variational simulation made with TAA software (which considers the parts deviation from their nominal dimension with an elastic model) and the results show a different deformation profiles, confirming that the elastic model is not suitable for tolerance stack-up of compliant parts.

Concluding, a simulation tool to better predict the distortions resulting from the assembly process it's still needed. The benefits of its application would be a more robust design and the reduction of adjustment cost during the ramp-up and manufacturing phases of a new product.

## 2 The proposed methods for simulating the B.i.W process modelling on shell mesh

To provide the basis for an improved variational analysis, this paper will focus on the central part of the coefficient influence method: the calculation of the part deformations, by FEM software, using a plastic material model and will provide the tools for the implementation of the RSW process, adapting the detailed results of the electric-thermal-mechanical study [9] to a shell element description of the assembly, so to reduce the model complexity and computational time.

Particular attention will be given to:

- the constraints,
- the deformation imposed by the weldgun,
- the contact management,
- the temperature imposition through the sheet thickness on the partition subjected to the welding spot.

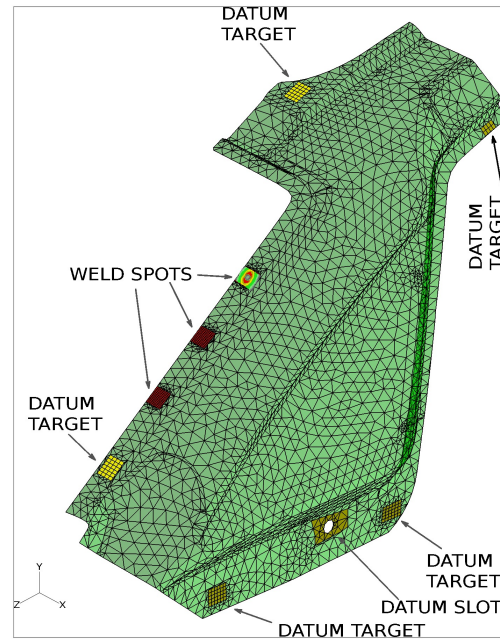


**Fig. 2** An example of a body side sheet metal part, meshed with shell elements, with datum targets and weld spots partitions.

### 2.1 Constraints

Figure 2 shows an example of a sheet metal part to be welded with other parts to form a larger body-side assembly. There, are highlighted the most important process information: the position of the datum targets and the weld spots.

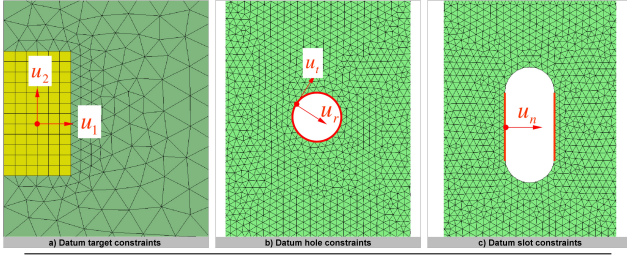
Correspondingly to those features, a mesh partition has been defined to locally specify a structured mesh of square elements and their dimension can be specified by the user. Outside those areas, the mesh will usually be defined by triangular elements, given the complexity of the free-form surfaces that are in this kind of parts.

This solution allows to choose independently the element dimensions of the datum or weld points and of the overall model, with the possibility of obtaining the best trade-off in terms of results approximation and computational time.

On datums will be enforced the constraints, as shown in figure 3.

Datum targets, once the fixture's clamps are closed, provide an encastre condition that can be defined constraining all the Degree of Freedom of the corresponding nodes in the FEM model. Holes and slot are to be constrained in the radial and normal direction respectively.

Commonly, to simplify the design and the manufacturing of fixtures, the designers develop proper embossments on the complex free-form surfaces, so to locally orient the holes and slots axis along the CAD assembly axis. Therefore, the radial and normal direction can be constrained with simple boundary conditions also in the FEM program.



Type	Constraint
Planar datum target area	$u_1 = u_2 = u_3 = 0$ $u_{R1} = u_{R2} = u_{R3} = 0$
Hole datume feature	$u_r = 0$
Slot datum feature	$u_n = 0$

**Fig. 3** Datum constraints.  $u_i$ : translations along assembly axis,  $u_{Ri}$ : rotations about assembly axis;  $u_r$ : hole radial direction;  $u_n$ : slot side normal direction.

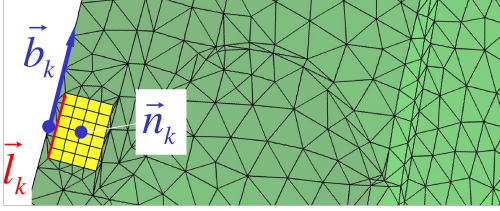


**Fig. 4** Orientation of datum target partition on mesh.

The information needed in the FEM system to define the partitions are: the coordinates of the datum target (2a), the datum target shape and dimensions (rectangular  $l \cdot w$ , square  $l$ , circular  $d$ ), the direction (2b) to orient one side  $\bar{l}_k$  of the non-circular shapes. The  $\bar{b}_k$  direction can be manually specified or by selecting a point and a border to align to, as shown in figure 4. The orientation condition of the border shape  $\bar{l}_k$  is given by (2c).

$$DT_k(x_1, x_2, x_3) \quad (2a)$$

$$\bar{b}_k(b_1, b_2, b_3) \quad (2b)$$

$$\bar{b}_k \cdot \bar{l}_k = 0 \quad (2c)$$

For those secondary datum targets, that are localized on welding flanges and so subjected to the form tolerance, it is possible to impose a displacement on the corresponding nodes in order to estimate the influence coefficients of the variation distribution on the sheet part caused by the fixture clamping.

Being  $\bar{n}_k = (n_1, n_2, n_3)$  the local normal of the datum target, the displacement components  $u_k$  are simply:

$$u_k = (T \cdot n_k) \cdot t \quad (3)$$

where  $T$  is the tolerance field and  $t \in [0; 1]$  the simulation step time, here applied as a progressive ramp function.

## 2.2 Weld spot deformation imposed by weld caps

In the previous work [9] the interaction of weldgun and sheets have been made with a model of two electrodes acting against the flanges' external sides with a surface-to-surface contact condition.

With the aim of eliminating the electrode models in the FEM assembly, a routine to define an analytical rigid surface with the electrode shape has been used.

Inside the routine it's necessary to determine if a point on the slave surface has penetrated the rigid surface, to define the local surface geometry by calculating the orientation for the constraint equations, friction directions and their rate of change as the point moves around on the surface. If the welding partition nodes and the rigid surfaces are in contact, the FE software will impose a constraint at the nodes to prevent overpenetration.

A common shape for the welding caps consists in a spherical extremity blending into a cone, but for the RSW application it never occur contact between the conical side of the caps and the sheet parts. So, with reference to figure 5 the cap geometry can be described as a sphere.

The coordinate of a node approaching the sphere can be written in cylindrical coordinates as:

$$r = \sqrt{x_1^2 + x_2^2} \quad (4a)$$

$$z = x_3. \quad (4b)$$

The interference  $h$  between the node and the spherical surface can be identified and evaluated by:

$$h = a - b \quad (5a)$$

$$b = \sqrt{r^2 + (z - z_Q)^2} \quad (5b)$$

The projection of the interfering point on the sphere surface is:

$$A' = (a \cos \beta \cos \gamma, a \cos \beta \sin \gamma, z_Q - a \sin \beta) \quad (6a)$$

$$\cos \gamma = \frac{x_1}{r} \quad (6b)$$

$$\sin \gamma = \frac{x_2}{r} \quad (6c)$$

For  $r = 0$ ,  $\gamma$  is not uniquely defined so it has been set to  $\gamma = 0$ . The tangents to the surface are:

$$\mathbf{t}^1 = (-\sin \beta \cos \gamma, -\sin \beta \sin \gamma, -\cos \beta) \quad (7a)$$

$$\mathbf{t}^2 = (-\sin \gamma, -\cos \gamma, 0) \quad (7b)$$

with a positive direction of  $\mathbf{t}^1$  and  $\mathbf{t}^2$  so that  $\mathbf{t}^1 \times \mathbf{t}^2$  defines an outward normal to the surface. The distance measure on the surface are

$$dS^1 = a d\beta \quad (8a)$$

$$dS^2 = a \cos \beta d\gamma \quad (8b)$$

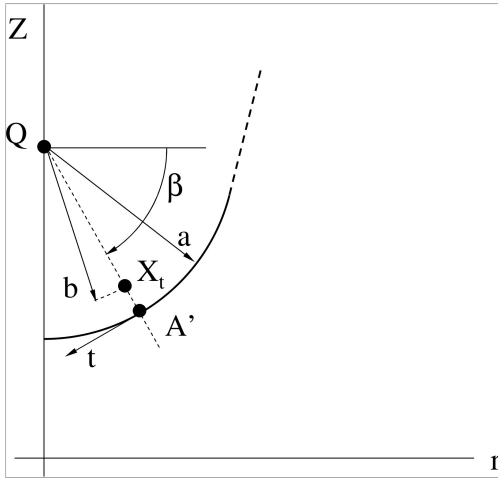


**Fig. 5** Geometrical description of analytical surface representing the weld caps.

so that the variation of the normal vector can be written as:

$$\frac{\partial \mathbf{n}}{\partial S^1} = \left( -\frac{1}{a} \sin \beta \cos \gamma, -\frac{1}{a} \sin \beta \sin \gamma, -\frac{1}{a} \cos \beta \right) \quad (9a)$$

$$\frac{\partial \mathbf{n}}{\partial S^2} = \left( -\frac{1}{a} \sin \gamma, \frac{1}{a} \cos \gamma, 0 \right) \quad (9b)$$

$$(9c)$$

This geometrical description of the spherical cap has been implemented in the RSURFU routine of Abaqus Standard [11], activating it by keyword editor and imposing a displacement to the reference point of the analytical rigid surface.

### 2.3 Sheet to sheet contact management for welded nodes

The aim is to manage the contact of the nodes of the flanges, during the spot welding operation, by changing the contact properties for those nodes who formed the weld nugget, to lock them together.

The behaviour that should be implemented can be described considering that during the weldgun closure phase, a contact pressure-overclosure relationship should be enforced with a frictional tangential behaviour and, after the cooling phase, the contact properties should be changed to prohibit the nodes separation and to ensure a rough tangential behaviour only for those nodes gone above the melting point.

But the position of the “melted” nodes on the contact partitions are not known in advance, because that depends on the mesh dimension and type (triangular or square).

With the standard options of FEM software, it's impossible to impose a different behaviour to those nodes because they cannot be distinguished “a priori” by the maximum temperature they reached.

An UINTER [11] routine has been developed to manage such behaviour. For the weldgun closure parts it has been implemented a softened contact form defined with an exponential law to make easier to resolve the contact condition:

$$p = 0 \quad h \leq -c \quad (10a)$$

$$p = \frac{p_0}{e-1} \left[ \left( \frac{h}{c} + 1 \right) \left( e^{\frac{h}{c+1}} - 1 \right) \right] \quad h > -c \quad (10b)$$

with  $c$  the initial distance,  $p_0$  a typical pressure for  $h = 0$ . During the closure step, the final contact pressures are saved into data blocks, by means of pointers and made available to all the routines by a COMMON statement [12].

At the end of the weldgun closure the contact forces between the surfaces are calculated and to ensure the force equilibrium during the weldgun opening, the  $p_0$  is rescaled and changed to the opposite sign:

$$\sum_i p_i A_i = \left| \sum_k p_k A_k \right| \quad (11)$$

where  $i$  is the index used to count all the nodes in the contact surfaces, while  $k$  is the index used to count the melted nodes, with  $k \ll i$ . Inverting this equation, for square mesh it's possible to rescale  $p_0$ .

Similarly the rough tangential behaviour has been implemented by a basic Coulomb friction model  $\tau = \mu p$  with a coefficient set to an high value to ensure the sticking condition.

This method allows a certain relative motion between surfaces, that has been restrained under an acceptable limit by manually adjusting the scaling coefficients. Its advantage is in allowing the enforcement of the main mechanical behaviour of the weld spot without knowing in advance nodes joined into the welded nugget.

### 2.4 Mesh offset to simulate the boundary condition for the unit displacement

The influence coefficient method has to be applied to each joint, where parts are usually welded on appropriate flanges, where each one is subjected to dimensional and geometrical tolerance and many weld spots.

So, it's necessary to consider each part in turn and to apply the unit displacement correspondingly to all the welding spots present, because using a plastic material model invalidate any linear behaviour.

To correctly determine the deformation of a part's flange it's necessary to “constrain” its movement, along the welding direction, considering that on the other side there will be the corresponding flange of the other part. But that cannot be obtained by mean of the standard Boundary Condition



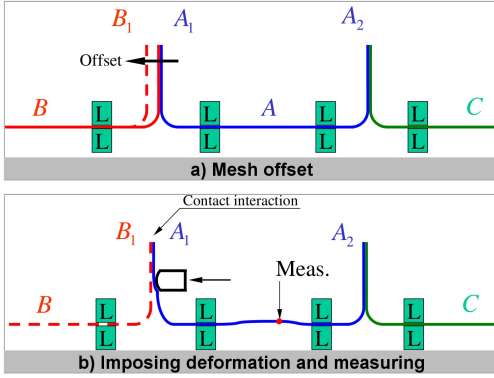


**Fig. 6** Management of welding boundary conditions. a) to the flange  $B_1$  being welded with  $A_1$  is given a thickness offset to simulate the unit displacement. b) to the flange  $A_1$  is imposed the electrode deformation that will force a contact with the offset  $B_1$  flange. The deformations are measured to define the influence coefficient matrix.

the FEM software usually provide for the complex geometry of the welding flanges.

The proposed solution consists in using the shell material offset on the parts surrounding the one on which the coefficient are being calculated.

In figure 6a is sketched the part subjected to the calculation:  $B$  and  $C$  will be welded to  $A$ . The weld flanges  $A_1$  and  $A_2$  of the part  $A$  will be welded in a known order with a known number of spots and will be subjected to a tolerance for which the influence coefficient are to be calculated.

Starting from the first welded flange  $A_1$  in its nominal dimension, the unit displacement is limited by offsetting the  $B_1$  opposing flange of the unit value and enforcing a surface contact interaction. After the imposition of the welding deformation and temperature cycle for all the spots on that surface, the deformation coefficient can be measured (figure 6b).

## 2.5 Temperature imposition on shell elements

The results of the model [9] regarding temperature distribution on welded parts, modelled with solid elements, are shown in figure 7 with reference to the sheet to sheet contacting faces, electrode to sheet contact surfaces, during the heating and cooling phases. It's evident the "heat sink" effect of the electrode. The results were computed for a standard butt joint presenting an initial gap due to part tolerances. The nodal results shown, can be easily exported as matrixes saved into a text file, imported into the FEA by means of an run-time routine and imposed to the nodes of the spot weld partition.

The coordinates of the points for which the temperature were calculated are saved in a local 2D coordinate system  $(u, v)$ , shown in figure 8, centred into the weld point position and for an extent corresponding to a rectangular partition of

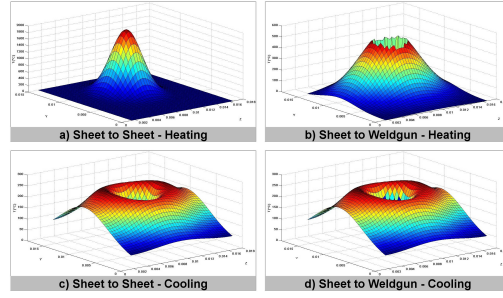


**Fig. 7** Calculated temperature distributions from [9].

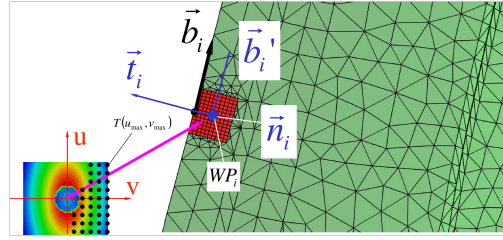


**Fig. 8** Temperature imposition on weld points partitions.

size  $(u_{max}, v_{max})$ , which is defined to include nodes with significantly high temperature. The figure also shows that the temperature distributions are not fully symmetrical and two principal axes can be found, due to the contact conditions of the surfaces.

The relevant geometrical properties of  $k$ -th spot weld partition are analogous to those described into section 2.1 for rectangular datum targets: the weld point position 12a, the unit vector normal to the surface 12b and an orientation vector 12c, to which the partition border  $\bar{l}_k$  is aligned 12d.

$$WP_k = (x_1, x_2, x_3) \quad (12a)$$

$$\bar{n}_k = (n_1, n_2, n_3) \quad (12b)$$

$$\bar{b}_k = (b_1, b_2, b_3) \quad (12c)$$

$$\bar{b}_k \cdot \bar{l}_k = 0 \quad (12d)$$

A local reference system can be calculated as follows:

$$\bar{t}_k = \bar{n}_k \times \bar{b}_k \quad (13a)$$

$$\bar{b}'_k = \bar{t}_k \times \bar{n}_k \quad (13b)$$

to guarantee an orthonormal set of direction  $(\bar{n}_k, \bar{b}'_k, \bar{t}_k)$ . To correlate the nodes belonging to the weld partition versus the temperature matrixes, their coordinates must be rotated into the matrix reference system. Let be  $N_k = (N_1, N_2, N_3)$  the coordinates of the nodes belonging to the weld partition passed to the routine; the Euler angles can be calculated as:

$$\alpha_k = \arccos \left( -\frac{n_2}{\sqrt{1-n_3^2}} \right) \quad (14a)$$

$$\beta_k = \arccos(n_3) \quad (14b)$$

$$\gamma_k = \arccos \left( \frac{b'_3}{\sqrt{1-n_3^2}} \right) \quad (14c)$$



When the  $Z$  axis of the two reference systems are aligned the transformation is managed with a simple rotation matrix around that axis.

Then the rotation matrix  $R_k = [R_\alpha R_\beta R_\gamma]$  is:

$$R_k = \begin{bmatrix} \cos \alpha & \sin \alpha & 0 \\ -\sin \alpha & \cos \alpha & 0 \\ 0 & 0 & 1 \end{bmatrix} \begin{bmatrix} 1 & 0 & 0 \\ 0 & \cos \beta & \sin \beta \\ 0 & -\sin \beta & \cos \beta \end{bmatrix} \begin{bmatrix} \cos \gamma & \sin \gamma & 0 \\ -\sin \gamma & \cos \gamma & 0 \\ 0 & 0 & 1 \end{bmatrix} \quad (15)$$

And the transformation is:

$$\begin{pmatrix} u \\ v \\ w \end{pmatrix}_k = [R]_k \begin{pmatrix} N_1 - x_1 \\ N_2 - x_2 \\ N_3 - x_3 \end{pmatrix} \quad (16)$$

In the local reference system,  $u_k$  and  $v_k$  are the coordinates of the welding partition node  $WP_k$  calculated by the routine. Assuming a local limited curvature of the surface,  $w_k$  can be neglected.

The nodes of the matrix surrounding  $WP_k$  can be calculated as:

$$u_k^{prec} = \text{INT} \left( \frac{u_k}{S} \cdot S \right) \quad v_k^{prec} = \text{INT} \left( \frac{v_k}{S} \cdot S \right) \quad (17)$$

$$u_k^{succ} = u_k^{prec} + 1 \quad v_k^{succ} = v_k^{prec} + 1 \quad (18)$$

being  $S$  the known mesh seed dimension.

Four flags variables are used to describe the closeness of the partition node to the matrix nodes:

$$\begin{cases} u_p^{coinc} = 1 & \text{if } |u_k - u^{prec}| < \delta \\ u_p^{coinc} = 0 & \text{otherwise} \\ u_s^{coinc} = 1 & \text{if } |u_k - u^{succ}| < \delta \\ u_s^{coinc} = 0 & \text{otherwise} \end{cases} \quad \begin{cases} v_p^{coinc} = 1 & \text{if } |v_k - v^{prec}| < \delta \\ v_p^{coinc} = 0 & \text{otherwise} \\ v_s^{coinc} = 1 & \text{if } |v_k - v^{succ}| < \delta \\ v_s^{coinc} = 0 & \text{otherwise} \end{cases} \quad (19)$$

For each direction, if the distance between two nodes is less than a  $\delta$  approximation factor, then the two nodes can be considered aligned in that direction.  $\delta = 10^{-5}$  m has been set to one hundredth of the sheet metal thickness magnitude. If there are two unit flags set, then the node can be considered coincident to a matrix node and the temperature value can be directly assigned. If it's present a coincidence only along one direction, then a linear interpolation is made. Otherwise a regression plane is used.

For each node it's calculated the temperature corresponding to the sheet to sheet interface and for the sheet to weld-gun interface, being this second value lowered by the heat sink effect of the electrode cooling. These two temperature values are imposed to the opposite integration point of the element and another linear interpolation is defined for the mid points, so to allow the out of plane bending of the shell caused by the temperature gradient, along the material thickness direction.

The node temperature matrixes were loaded into the Abaqus Standard solver by mean of the UEXTERNALDB [11] routine, which allow the access to external files at the beginning of the analysis. The values were stored into COMMON Fortran [12] variables so to make them accessible to all the

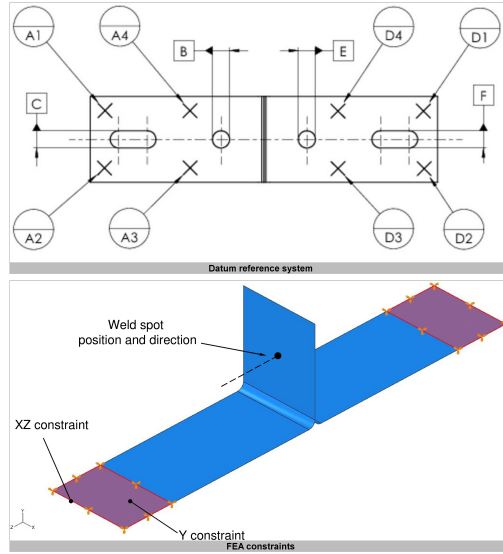


**Fig. 9** a) Datum reference system for the fixturing. b) Constraints simulated in the FEA.

other routines. And, finally, the UTEMP routine [11] has been used to implement the calculation of the temperatures for the welding point partition as stated above.

The important property of this set-up is the independence from the mesh dimension and element shape chosen the weld partition.

### 3 Experimental validation and results analysis

The methods defined in the previous section have been tested on a simple assembly consisting of a butt joint on which the datum reference system has been simplified as an incastre condition on the rear side of each part, as implemented in [9] and here shown in 9

To simulate the gap condition caused by tolerances and obtaining the influence coefficient, the material thickness of the left weld flange has been offset of a unit quantity and the analytical rigid surface routine has been used to simulate the welding closure. Figure 10a shows the initial condition while 10b show the effect of the contact of the deformed flange against the offset one, magnified two times. Figure 10c shows the shell to shell deviation computed between the current method's results and the results of a standard simulation performed on shell elements with the welding caps explicitly modeled. The results shows an acceptable agreement of the two solutions, being the deviation under 0.05-mm, along the welding direction and the vertical deviation under 0.1 mm. Figure 10d represents the deformed shape obtained by the use of the routine, magnified ten times.

Figure 11 shows the result of the contact management made with the run time routine. During the weldgun release, the contact pressure of the nodes forming the welding

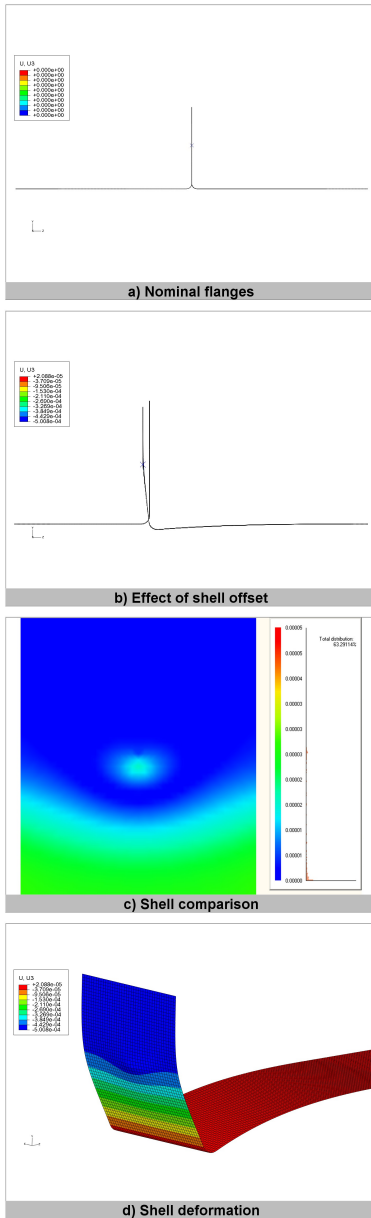


**Fig. 10** a) Initial condition. b) Effects of the shell offset to simulate the tolerance. c) Comparison of the results of the analytical rigid surface routine with a standard simulation (shell to shell deviation [m]). d) Nodal displacement [m] along welding direction of flange deformed by routine.

nugget is reversed, so to maintain the sheet closed against the actions of springback and the contact pressure of the nodes surrounding the nugget.

Finally, figure 12 shows the results of the application of temperature imposed by routine on the external nodes of the shell flange. The deviation of the result from the original values obtained in the complete 3D simulation [9] are negligible.

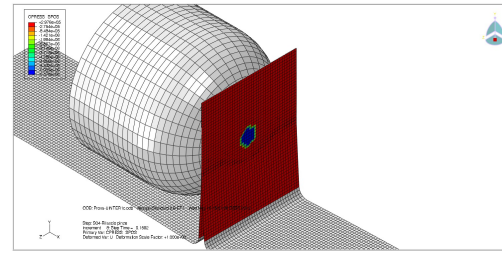


**Fig. 11** Contact pressure after electrode force releasing. Correspondingly to the nodes forming the welding nugget, the contact pressure is set negative, to simulate the joint.

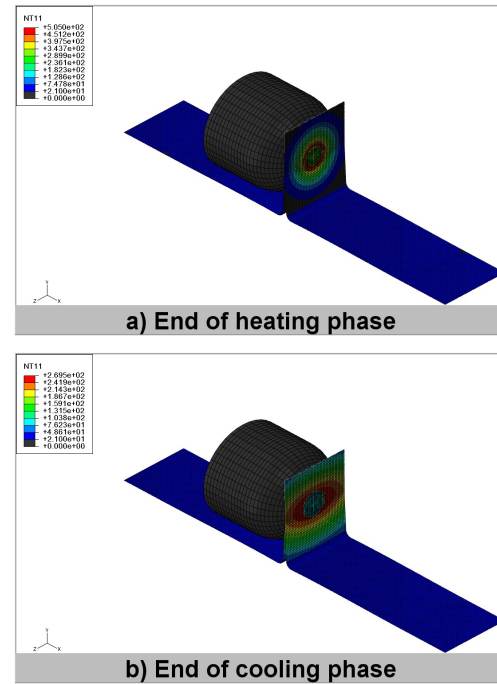


**Fig. 12** Results of temperature imposition on the flange's external nodes [°C]: a) at the end of the heating step, b) at the end of the coolign step.

## 4 Conclusions

The methods here delineated allows the calculation of the influence coefficient necessary for a variational analysis on compliant assemblies, considering the main aspects of the welding and fixturing processes and implementing them on a shell model, without recurring to complex co-simulation.

The temperature distribution calculated along the thickness of a 3D model are imposed on the integration point of the shell elements, during the heating and cooling phases, so to provide the thermal dilatation and to change the material plastic properties as temperature function.

The effect of weldgun closure on welding flanges is provided through an analytical surface routine definition, so to eliminate the the explicit modelling and positioning of the welding cups for each weld location.

The correct boundary condition of weld spots, while applying the unit displacement to the weld partition is defined by the mesh offset parameter to the flange of the corresponding mating part.

To simulate the weld spot joint an interaction routine has been adapted to prohibit the opening and tangential slip of only those nodes who reached a temperature above the melting point.

## References

1. Chase K, Parkinson A (1991) A survey of research in the application of tolerance analysis to the design of mechanical assemblies. *Research in Engineering Design* 3(1):23-37. DOI:10.1007/BF01580066.
2. Maropoulos P-G, Ceglarek D (2010) Design verification and validation in product lifecycle. *CIRP Annals – Manufacturing Technology* 59(2):740-759. DOI:10.1016/j.cirp.2010.05.005.
3. Liu S-C, Hu S-J (1997) Variation simulation for deformable sheet metal assemblies using finite element methods. *ASME Journal of Mfg. Science and Engg.* 119:368-374.
4. Byungwoo L, Shalaby M-M, Collins R-J, Crisan V, Walls S-A, Robinson D-M, Saitou K (2007) Variation Analysis of Three Dimensional non-rigid Assemblies. *IEEE International Symposium on Assembly and Manufacturing ISAM '07* 05(05):13-18. DOI:10.1109/ISAM.2007.4288442
5. Feulvarch E, Robin V, Bergheau J-M (2004) Resistance spot welding simulation: a general finite element formulation of electrothermal contact conditions. *Journal of Materials Processing Technology* 153-154:436-441. DOI:10.1016/j.jmatprotec.2004.04.096.
6. Hou Z, Kim I, Wang Y, Li C, Chen C (2004) Finite element analysis for the mechanical features of resistance spot welding process. *Journal of Materials Processing Technology* 185(1-3):160-165. DOI:10.1016/j.jmatprotec.2006.03.143.
7. Ranjbar Nodeh I, Serajzadeh S, Kokabi A-H (2007) Simulation of welding residual stresses in resistance spot welding, FE modeling and X-ray verification. *Journal of Materials Processing Technology* 205(1-3):60-69. DOI:10.1016/j.jmatprotec.2007.11.104.
8. Eisazadeh H, Hamed M, Halvae A (2010) New parametric study of nugget size in resistance spot welding process using finite element method. *Materials & Design* 31(1):149-157. DOI:10.1016/j.matdes.2009.06.042.
9. Moos S, Vezzetti E (2011) Compliant assembly tolerance analysis: guidelines to formalize the resistance spot welding plasticity effects. *The International Journal of Advanced Manufacturing Technology*, Springer London, 0268-3768. DOI: 10.1007/s00170-011-3729-0
10. Fan X, Masters I, Roy R, Williams D (2007) Simulation of distortion induced in assemblies by spot welding. *Proceedings of the Institution of Mechanical Engineers – Part B: Journal of Engineering Manufacture* 221(8):1317-1326. DOI:10.1243/09544054JEM782
11. ABAQUS. ABAQUS v6.9ef1 online documentation, Abaqus User Subroutines Reference Manual.
12. Nyhoff L, Leestma S (1997) *Fortran 90 for engineers and scientists* Upper Saddle River: Prentice-Hall.